Marquette University

e-Publications@Marquette

Electrical and Computer Engineering Faculty Research and Publications/College of Engineering

***This paper is NOT THE PUBLISHED VERSION;* but the author's final, peer-reviewed manuscript.** The published version may be accessed by following the link in the citation below.

Proceedings of SPIE 8973: Micromachining and Microfabrication Process Technology XIX, No. 8973 (March 2014). DOI. This article is © Society of Photo-optical Instrumentation Engineers (SPIE) and permission has been granted for this version to appear in e-Publications@Marquette. Society of Photo-optical Instrumentation Engineers (SPIE) does not grant permission for this article to be further copied/distributed or hosted elsewhere without the express permission from Society of Photo-optical Instrumentation Engineers (SPIE).

Phase Change Materials (PCM) Fabricated in Vertical Structures for Reconfigurable and Tunable Circuits

Edwardo Barajas
Air Force Institute of Technology
Ronald A. Coutu
Air Force Institute of Technology

Abstract

Germanium Telluride (GeTe) can be described as a non-volatile (latching state) phase change material (PCM) in memory applications. GeTe also exhibits a volatile (reversible state) region when heated and cooled between 100-180 °C. At temperatures higher than 185 °C the material crystallizes and "latches" until a temperature near to its melting point (725 °C) is reached and cooled rapidly (quenching). Germanium Antimony Telluride (GeSbTe) or also known as GST has similar characteristics as GeTe. GST also exhibits a volatile (reversible state) region when heated and cooled between 100-150 °C. GST crystallizes at 155 °C and its melting point is 600 °C. This paper demonstrates the feasibility of fabricating radio frequency (RF) devices of phase change materials (PCM) and it also presents a comparison between amorphous and crystalline PCMs in the RF spectrum. Previous work focuses on exploiting GeTe and GST as nonvolatile materials in memory applications, and also on characterizing them for their electrical and mechanical properties. The approach here focuses on fabricating RF devices and

analyzing their responses. A simulation with resistor-capacitor (RC) and resistor-inductor (RL) circuits is presented to represent the response of the RF devices under testing. The fabrication process includes two-layer and four-layer devices on the Si wafer. PCMs are sputtered and the test pads are deposited using electron beam evaporation. Results show that these RF devices alone can serve as a low pass filter with a cutoff frequency of 10 MHz.

1. INTRODUCTION

Currently, switching of complex systems is achieved by using active electronics components (semiconductor-based diodes or transistors) or microelectromechanical systems (MEMS).[1] Unfortunately these systems are limited by the power consumption and non-linear behavior of the semiconductor components, or by the yet-to-be-proven reliability of MEMS switches and variable capacitors.[2,3] Current research is directed towards the development of smart multifunctional materials with novel and improved properties that may be viable solutions for electronic devices with greater functionality, faster operating speed, and reduced size.[2]

Phase change materials (PCM) or metal insulator transition (MIT) materials are materials that change from an amorphous state to a crystalline state when external energy is applied.[4] The atomic structure is rearranged during this transformation. In the amorphous state the atoms are scattered and randomly arranged, whereas in the crystalline state the atoms maintain a pattern and are neatly arranged forming lattice structures.[5] In the amorphous state, the material behaves in a manner similar to a semiconductor, showing high resistivity across the material. In the crystalline state the material behaves similar to a conductor, with low resistivity. The ability to shift resistivity that occurs upon state transitions can be used in many applications, such as: a solid state low pass filter, solid state switch and reconfigurable circuits. The solid state low pass filter is the primary application of interest in this paper.

2. DESIGN

The purpose of this research is to test a variety of MEMS-device configurations formed with layers of PCMs to understand their behavior in micro sized devices. The micro-test structures are fabricated using four different masks. These masks are laid out using the MEMS Pro software and subsequently fabricated using the Heidelberg mask maker in the AFIT's class 1000 clean room. The layout includes vertical structures, control structures and circuits. Vertical structures are four-layer devices and control structures are two-layer devices. **Figure 1** shows the complete design of the four masks stacked sequentially to illustrate the finalized device configuration. Pointing with arrows the zoom-in devices are shown to the side of the mask.

Figure 1: Layout of the four masks on using MEMS Pro L-Edit software. Each area has been magnified to better illustrate the devices.

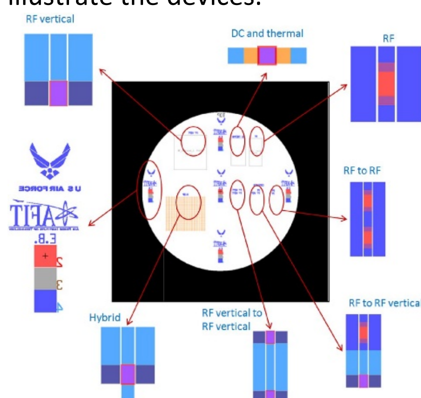

The purpose of the separate designs are to test different features of PCMs. RF devices, as the name suggests, test the radio frequency (RF) phase change capability of PCMs. DC devices are utilized to test the phase change ability of PCMs under the influence of DC current. Thermal devices are available for simply measuring the phase change capability of the PCM with a directly applied thermal stimulus.

Part of the design is the modeling and simulation of the low pass filter that is expected as a result of the responses thorough the RF devices. **Equation 1** and **equation 2** describe the transfer function and cutoff frequency, respectively, of a low pass filter.[6]

$$\frac{Vout(s)}{Vin\ (s)} = \frac{\frac{1}{CR}}{s + \frac{1}{CR}} \tag{1}$$

$$f_c = \frac{1}{2\pi RC} \tag{2}$$

Where R is the resistance, C is the capacitance and f_c is the cutoff frequency.

3. FABRICATION

Figure 2 illustrates a step-by-step fabrication process for patterning the PCM test structures onto a wafer. The fabrication process starts with a bare Si wafer and step #1 deposits a layer of 230 nm silicon nitride (Si_3N_4). This Si_3N_4 layer serves as an electrical insulation layer between the wafer and the devices.[7] The first layer of devices is deposited through a lithographic process and mask 1, illustrated in step #2. Step #3 deposits a layer of titanium (Ti) and gold (Au) using evaporation. The purpose of this layer is to create probe pads for future testing. Another layer of photo resist is deposited in step #4 and mask 2 is used to pattern the second layer of devices for which step #5 deposits sputtered PCM. Steps #6 deposits another layer of photoresist and mask 3 patterns the leveling block for devices. Step #7 deposits a top layer of Au using evaporation. Step #8 deposits another layer of photoresist and mask 4 patterns the fourth layer on the devices. Step #9 deposits the fourth layer of Ti and Au using electron beam evaporation. Step #10 and #11 are optional if photoresist walls are desired.

Figure 2: The fabrication process with steps. Each cross-sectional fabrication step is shown below the appropriate mask.

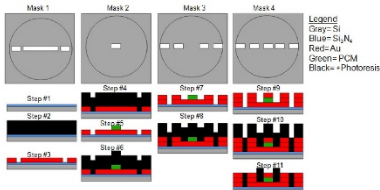

Figure 3 shows the result of the device fabrication process explained above. These devices are divided into four different quadrants on the wafer. The first quadrant contains RF vertical structures. The second quadrant contains RF, DC and thermal devices. The third quadrant is dedicated to circuits: RF devices in series, RF devices or vertical structures in series, DC vertical structures in series and parallel.

The fourth quadrant is dedicated to hybrid structures. The purpose of the hybrid structures is to combine all devices into one type of structures in order to make the testing easier.

Figure 3: Wafer with devices in the four quadrants. All devices are finished and ready for testing.

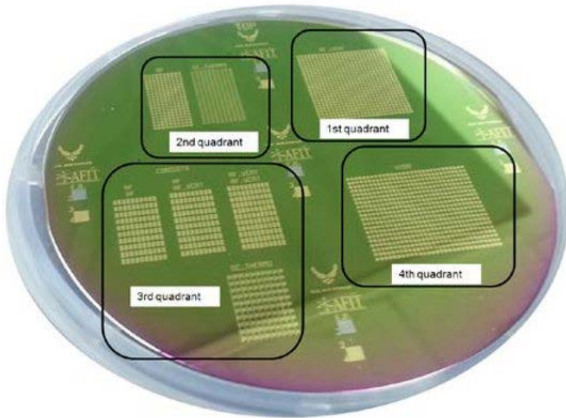

4. TEST

Initially, witness samples are thermally tested to confirm the behavior of the PCM is as predicted. PCM resistance is dependent on temperature; therefore when the PCM transitions the resistance is directly affected. Resistance of the witness samples is measured using an ohmmeter while the sample is being heated from 20 °C – 200 °C using a thermally controlled stage. In order to take the measurements, the measurement probes must be carefully placed on the respective probe sites on each device. Following the initial thermal testing, and RF signal is utilized in an attempt to transition the RF PCM devices. RF device testing is achieved using a radio frequency programmable network analyzer (PNA) and a probe station. The RF PNA uses two ground-signal-ground probes, with the surrounding ground lines used to better isolate the signal line from noise. The RF PNA measures the S_{11}, S_{12}, S_{22} and S_{21} signals on the RF devices. The S_{11} measures the input impedance signal, the S_{12} measures the signal from channel 1 to channel 2, the S_{22} measures the output impedance signal and the S_{2J} measures the signal from channel 2 to channel 1. In a few words, the S_{11} and the S_{22} represent the reflection back to the same channel, and the S_{12} and the S_{21} represent the transmission from one channel to the other. The J Micro probe station and the Agilent E8362C RF PNA were used to measure frequency signals from 10 MHz to 20 GHz range. **Figure 4** shows the J Micro Technology probe station and the Agilent E8362C PNA used to take these readings.

Figure 4: RF probe station connected to the PNA. The RF probes are use to measure the RF response of the RF devices.

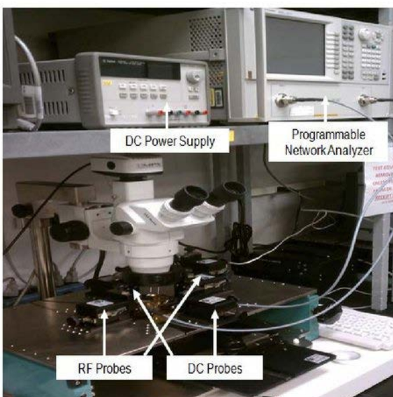

5. RESULTS

During the initial fabrication process layers of Copper (Cu) were used on the first layer and third layer but it was discovered that Cu oxidizes very rapidly and creates a layer of copper oxide that prevents good adhesion of subsequent layers. All vertical structures (four-layer devices) are shorted from the bottom electrode to the top electrode. This short circuiting can be attributed to pinholes on the PCM.

Thermal testing indicated that the PCM behaved as expected in that the material displayed a drastic change in resistance. **Figure 5** shows a transition plot for GeTe, in which it can be seen that the transition temperature is between the range of 180°C and 190°C. The actual transition temperature of GeTe was found to be 185°C. The resistance changes from 4.92×10^6 in the amorphous state at 20°C to 106.5 Ω in the crystalline state at 250°C. The resistance value drops by four orders of magnitude and the dynamic range was found to be 18028 X. Dynamic range of a PCM is the ratio of the resistance at the amorphous state over the crystalline state. Previous research showed a GeTe dynamic range of 7×10^3 X.[8]

Figure 5: Transition temperature of GeTe witness samples. The cursor labels point out the temperature and resistance before and after transition.

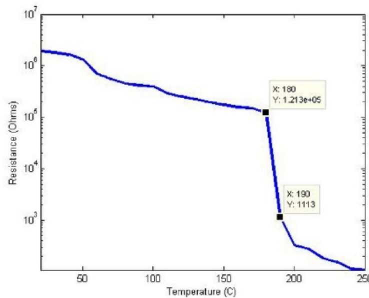

Figure 6 shows a transition plot for GST, in which it can be seen that the transition temperature lies between the range of 150 °C and 160 °C. The actual transition temperature of GeTe was later found to be 155 °C. The resistance changes from 6.37×10^7 in the amorphous state to 3675 Ω in the crystalline state. The resistance value drops by four orders of magnitude and the dynamic range was found to be 17333 X. Previous research showed a GST dynamic range of 70 X.[8]

Figure 6: Transition temperature of GST witness samples. The cursor labels point out the temperature and resistance before and after transition.

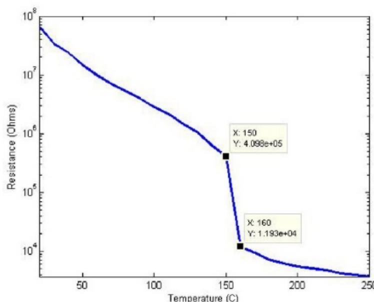

The RF measurements of amorphous GeTe and crystalline GeTe are shown in **Figure 7** and **Figure 8** respectively. The reflection (S_{11} and S_{22}) of the amorphous devices is unchanged throughout the range of the PNA. The reflection of the crystalline devices starts at -9 dB and converges to 0 dB at 3 GHz. The difference in reflection from amorphous to crystalline is negligible because the fluctuation from 0 to -9 dB of the crystalline devices can be attributed to electrical noise.

Figure 7: RF measurements of amorphous GeTe devices. The legend identifies each S parameter according to color.

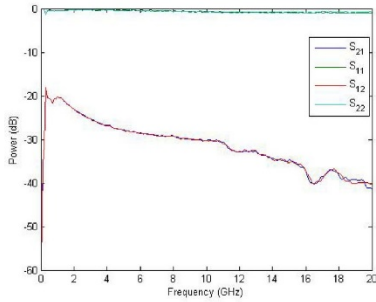

Figure 8: RF measurements of crystalline GeTe devices. The legend identifies each S parameter according to color.

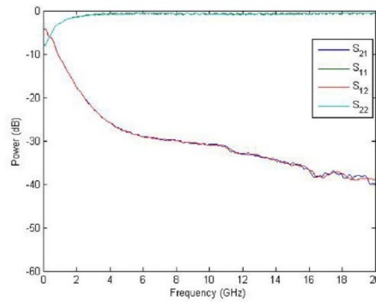

The interesting phenomenon occurs in the transmission (S_{12} and S_{21}). The transmission of amorphous devices starts at - 65 dB at 10 MHz and quickly moves up to -20 dB at 1 GHz, and then slowly decreases to -40 dB at 20GHz. The response of the amorphous devices blocks frequencies in the range of 10 MHz to 20 GHz. The transmission of crystalline devices starts at -4 dB at 10 MHz and moves down to -30 dB at 5 GHz, and then slowly decreases to -40 dB at 20 GHz. This latter response is interesting because the signal represents a low pass filter, where frequencies from 10 MHz to 5 GHz passed with minimum losses.

Simulation reveals a similar response with a resistor-capacitor (RC) or resistor indictor (RL) circuit to form a low pass filter. **Figure 9** shows a low pass filter obtained using simulation. The calculated values for R and C are 160 Ω and 100 pF respectively. The transfer function that produces this filter is shown in **Equation 1** and the cut-off frequency is shown in **equation 2**. For sake of simplicity only the RC low pass filter and their respective elements are mentioned here, however the RL low pass filter generates a similar response.

Figure 9: Low pass filter with cutoff frequency of 10 MHz.

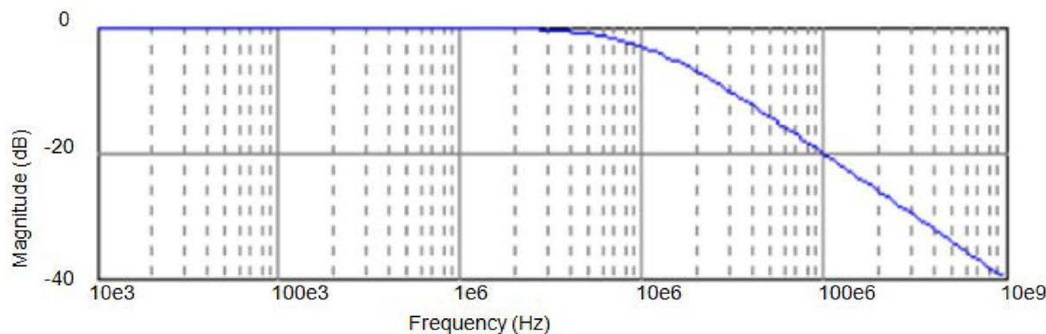

Figure 10 and **Figure 11** show the RF measurements of the amorphous GST and crystalline GST, respectively. The RF responses of GST are not significant because there is not a difference between the amorphous GST to the crystalline GST.

Figure 10: RF measurements of amorphous GST devices. The legend identifies each S parameter according to color.

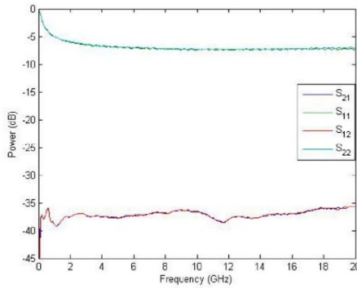

Figure 11: RF measurements of crystalline GST devices. The legend identifies each S parameter according to color.

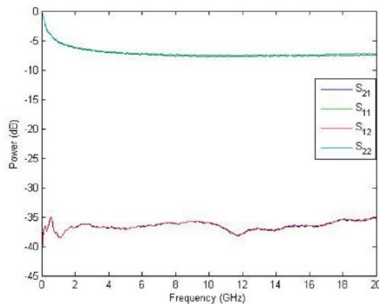

6. CONCLUSIONS

Micro-devices utilizing PCM were designed and fabricated using basic MEMS fabrication process. The purpose of the devices was to understand the behavior of PCMs and ultimately create a single element low pass filter. PCMs were tested using witness samples to characterize transition temperatures. The GeTe witness sample transitioned at lower temperatures than the GST witness samples. Devices were initially tested using DC signals; unfortunately all vertical devices were shorted from the bottom electrode to top electrode. Subsequent testing centered on measuring the RF capabilities of the devices in both the crystalline and amorphous state. The RF response of GeTe devices shows a significant difference from amorphous to crystalline; where as the RF response of GST devices don't change. This paper shows that RF GeTe devices can be used as a low pass filter without the need of any other elements.

Acknowledgments

The authors would like to thank the Air Force Research Laboratory (AFRL) Sensors for their assistance, use of their resources, and facilities. The authors also thank the technical support and dedicated work of AFIT's own cleanroom staff, Rich Johnston and Thomas Stephenson.

Disclaimer: The views expressed in this article are those of the authors and do not reflect the official policy or position of the United States Air Force, Department of Defense, or the United States Government.

REFERENCES

[1] D. M. Pozar, Microwave Engineering, Wiley & Sons, 2005.Google Scholar

[2] A. Crunteanu, J. Givernaud, P. Blondy, J.-C. Orlianges, C. Champeaux and A. Catherinot, “Exploiting the semiconductor-metal phase transition of VO2 materials: a novel direction towards tuneable devices and systems for RF-microwave applications,” in Advanced Microwave and Millimeter Wave Technologies, Rijeka, Croatia, InTech, 2010, pp. 35–53.Google Scholar

[3] G. M. Rebeiz and J. B. Muldavin, “RF MEMS Switches and Switch Circuits,” IEEE Microwave Magazine, pp. 59–71, 2001. **10.1109/6668.969936**Google Scholar

[4] A. Pergament, “Metal-Insulator Transition: The Mott Criterion and Coherence Length,” Journal of Physics: Condensed Matter, vol. 15, no. 19, p. 3217, 2003.Google Scholar

[5] M. Surface, “Photovoltaics: The Encyclopedia of Earth,” 24 April 2010. [Online]. Available: **www.eoearth.org/article/Photovoltaics**. [Accessed 21 November 2012].Google Scholar

[6] R. S. Muller, T. I. Kamins and M. Chan, Device Electronics for Integrated Circuits, New York: Wiley, 2003.Google Scholar

[7] G. S. May and S. M. Sze, Fundamentals of Semiconductor Fabrication, Hoboken, New Jersey: John Wiley & Sons, Inc., 2004.Google Scholar

[8] E. K. Chua, L. P. Shi, R. Zhao, K. G. Lim, T. C. Chong, T. E. Schlesinger and J. A. Bain, “Low resistance, high dynamic range reconfigurable phase change switch for radio frequency applications,” Applied Physics Letters, vol. 97, no. 18, 2010. **10.1063/1.3508954**Google Scholar